Acta Oceanol. Sin., 2022, Vol. 41, No. 1, P. 132–140
https://doi.org/10.1007/s13131-021-1741-2
http://www.aosocean.com
E-mail: ocean2@hyxb.org.cn

Analysis of the inter-annual variability and southward expansion of red tides in the Zhejiang coastal waters from 1981 to 2018

Lili Xu[1, 2], Yinyu Liang[1, 2*], Wenjun Xiao[1, 2], Bingrui Chen[1, 2]

[1] East China Sea Marine Forecast Center of the State Oceanic Administration, Ministry of Natural Resources, Shanghai 200136, China

[2] Key Laboratory of Marine Ecological Monitoring and Restoration Technologies, Ministry of Natural Resources, Shanghai 200081, China

Received 23 September 2020; accepted 8 October 2020

Abstract

A time series dataset spanning 39 years (1981–2018) on red tide events in Zhejiang coastal waters was used to study the characteristics of inter-annual spatial and temporal variations. A distinct inter-annual pattern characterized by low frequency, explosive growth and fluctuating decline stages was found over the studied time scale. Most red tide events occurred in parallel to the bathymetric contour, and 95.4% were located to the west of the 50 m isobath. Additionally, the high-incidence area of red tides is expanding southward. In this paper, local sea surface temperature (SST), mariculture area and secondary industry growth rate are introduced and identified as the main factors influencing the nutrient and hydrometeorological conditions. A multivariate nonlinear regression equation based on these factors was constructed, and the goodness of fit coefficient was 0.907. The causes of the annual variation and high-frequency area in the southward expansion were quantitatively analyzed based on the proposed regression model. Finally, the results indicated that 68.7% of the annual occurrence variation of red tide was due to the SST and mariculture area, which are the main impact factors; however, secondary industry growth could compensate for the nutrient deficiency caused by the sharp mariculture area reduction and decreased SST. The background nutrient level, which is elevated by coastal economic development, especially secondary industry, is the main determinant of the southward expansion. Although the trend of the southward expansion of high-frequency areas has not changed, the red tide frequency in coastal cities has decreased by half and remained at a stable level after 2010 due to substantial economic restructuring and environmental protection.

Key words: Zhejiang Province, red tide, peak drop, inter-annual variation, southward expansion

Citation: Xu Lili, Liang Yinyu, Xiao Wenjun, Chen Bingrui. 2022. Analysis of the inter-annual variability and southward expansion of red tides in the Zhejiang coastal waters from 1981 to 2018. Acta Oceanologica Sinica, 41(1): 132–140, doi: 10.1007/s13131-021-1741-2

1 Introduction

Red tide, termed as harmful algal blooms (HABs), refers to the phenomenon of discoloration of seawater caused by the excessive accumulation of marine plankton biomass. Especially frequent in recent years, red tide is one of the worst ecological disasters in the coastal waters in China, posing a serious danger to the marine ecological environment, fishery production, human life and social economy. The combination of the effects of upwelling currents when diluted water rushes southward from the Changjiang River and warm currents from Taiwan flow northward, the presence of a suitable environment with regular marine dynamic interaction, and the availability of rich nutrients is beneficial to the growth and outbreak of red tide organisms in the Zhejiang coastal waters. Over the past few decades, concentrations of nitrogen and phosphorus in the seawater have been significantly higher due to human activities; consequently, red tides occur more frequently than in other parts of the China seas. In the last few decades, the outbreaks of red tide in the Zhejiang coastal waters have increased to nearly 50% of the total number in China (Xu et al., 2013). Especially since the 21st century, large-scale red tides and toxic red tides have been increasing, which is harmful to marine ecological environmental protection and the high-quality development of the marine economy in the Zhejiang Province.

Research on red tide has been performed in China for a long time. In the 1980s, the mechanism of red tide on the southeastern coast of China was studied (Qi, 2003). Currently, red tide is being studied primarily with four methods, namely, analysis of the spatial and temporal distribution of red tide (Guo et al., 2015; Wei et al., 2012; Gao et al., 2017), the mechanism of red tide occurrence or algal species growth (Liu et al., 2011; Chen et al., 2013; Wen et al., 2009), the technological innovation of red tide field and remote sensing monitoring (Zhao et al., 2005; Zhao et al., 2003), and the simulation and prediction of the red tide outbreak with ecological dynamics models or big data technology (Jing et al., 2008; Lin, 2011; Feng et al., 2007; Wang et al., 2006). Among them, studies on the spatiotemporal variation of red tide have mainly been performed to assess the short-term seasonal or

Foundation item: The National Basic Research Program of China under contract No. 2016YFC1401900; the Open Research Funds of Key Laboratory of Marine Ecological Monitoring and Restoration Technologies under contract No. MATHAB201703.
*Corresponding author, E-mail: liangyinyu@ecs.mnr.gov.cn

long-term interdecadal changes (Zhang, 2013; Long et al., 2008; Song et al., 2018; Li, 2012). For instance, Yang and He (2009) discovered that the frequency of red tide in the China seas is higher in the year following an El Niño events. Deng et al. (2017) analyzed the relationship between the occurrences of red tide and the ENSO index in the East China Sea from 1981 to 2011 and preliminarily noted that 2000 was the turning point without explaining the reason. He and Yang (2009) found that the ENSO index was moderately correlated with the frequency of red tide events in the East China Sea at certain times. Although the interannual variation law of red tides has been studied in the above research, few studies have assessed the impact factor and mechanism of the spatiotemporal variation of red tide in the Zhejiang coastal waters, which feature the most serious red tide disasters.

In this study, based on data on 711 red tide events from 1981 to 2018 in the Zhejiang coastal waters, the temporal variation and spatial distribution of red tides were systematically analyzed. The main impact factors of red tide occurrence were statistically analyzed. Based on these factors, a physical mathematical model considering the local sea surface temperature, mariculture area and land-sourced pollutant emissions was established. The effects of changes in natural environmental factors, such as the local sea surface temperature (SST) and upwelling, and human activities on red tide events were discussed. We also aimed to quantitatively explain the driving force of inter-annual variations of the three stages and southward expansion of high-frequency areas of red tide to provide technical support for red tide monitoring, early warning, prevention and disposal decision-making in the Zhejiang coastal area.

2 Materials and methods

2.1 *Data sources*

Information on red tide events, hydrometeorology, the marine environment and socio-economic development indicators, which are closely related to long-term red tide changes in the Zhejiang coast waters, was systematically collected and organized. Due to multiple reforms of local institutions, the weakness of monitoring techniques and insufficient funding for scientific research, information on the restoration of red tide events is the most complex among these data.

In this study, the red tide event was defined as discolored water caused by a high biomass of phytoplankton in a marine habitat, and the monitoring dataset included time, location, maximum area and other elements. A red tide time-series dataset from 1981 to 2006 was collected and reorganized by the Zhejiang Ocean Monitoring and Forecasting Center, which is managed by the Zhejiang Natural Resources Department. The dataset from 2007 to 2015 was provided by the Zhejiang Ocean Monitoring and Forecasting Center as well. The monitoring dataset from 2016–2018 was provided by the East China Sea Monitoring Center, which is managed by the East China Sea Bureau of the Ministry of Natural Resources. Local county annals and other references (Zhao, 2010) were also used for data collection, compilation, quality control and verification. Thus, overall, a dataset including 711 red tide events from 1981 to 2018 in the Zhejiang coastal waters was constructed.

The hydrometeorological factors used in this study include the ENSO index and SST. The ENSO indexes during 1981–2018 originate from NOAA. The SST from 1981–2018 recorded at the south and north ends of the Zhejiang coastal waters originated from Nanji Station (27.41°N, 121.1°E) and Shengshan Station (30.7°N, 122.81°E), respectively, of the National Global Ocean Stereoscopic Observation Network of Donghai Bureau. The SST refers to the sea water temperature between the sea surface and 0.5 m depth and is expressed by the average observation data values at 8:00, 11:00, 14:00 and 17:00 from the artificial observation station according to the *Specification for Coastal Observation* (GBT 14914–2006).

The marine water quality related to the "proportion of class IV to classes less than IV" from 2000 to 2018 that was published in the *Zhejiang Marine Environmental Bulletin* is released by the Department of Ecology and Environment of Zhejiang Province.

Finally, gross domestic product (GDP), industrial added value index and mariculture area were introduced as indicators with a high relationship between red tide occurrence and social and economic development of Zhejiang Province. The datasets were produced based on the statistical yearbook released by the Ningbo and Wenzhou. Table 1 presents a statistical summary of the data.

2.2 *Methods of statistical analysis*

Both rank correlation and multivariate nonlinear regression analysis were used to identify and examine the sector-based effects of red tide occurrence and were performed using the 25th version of Statistical Product and Service Solutions (SPSS) software program.

2.2.1 *Rank correlation analysis*

The method of rank correlation analysis was first used to analyze the priority of the correlation between these factors, such as hydrometeorology and marine environment, and the occurrence of red tide, which has the advantage of not being limited by the preconditions, such as the overall distribution of variables, the number of samples or whether the correlation is linear. This method is a nonparametric statistical method as long as it satisfies the condition that the change trend of variables is similar or one variable can be expressed as a monotonic function of another, which has a wide range of applications. The Spearman correlation coefficient is one of the commonly used rank correlation analysis methods, as shown below:

$$\partial = \frac{\sum_{i=1}^{n} \left(X_i - \overline{X}\right)\left(Y_i - \overline{Y}\right)}{\sqrt{\sum_{i=1}^{n} \left(X_i - \overline{X}\right)^2} \sqrt{\sum_{i=1}^{n} \left(Y_i - \overline{Y}\right)^2}}, \tag{1}$$

where n represents the number of samples; i is the number of introduced factors; X is the independent variable; and Y is the dependent variable.

2.2.2 *Multiple nonlinear regression*

A multifactor model of red tide occurrence was constructed using the multivariate nonlinear regression method, which is used to analyze and study the temporal and spatial variation law of red tide occurrence. Moreover, the core idea of multivariate nonlinear regression is to construct polynomial functions, and its parameter estimation is the key step. Here, the Gaussian-Newton method was used for parameter estimation, and Taylor's series expansion was performed for the expected function, resulting in iterative solutions. For more details on this method, see below.

Goodness of fit coefficient of a multivariate nonlinear regression equation:

Table 1. List of the main impact factors that are closely related to the long-term change of red tide

Data category	Data record elements	Data cycle	Domain or station	Specifications or technical standards	Notes on information
Red tide events	time, location, maximum area, dominant species	1981–2015	Zhejiang coastal waters	technical specifications for red tide monitoring(HY/T069–2005)	dataset from 1981 to 2006 is reorganized by the Zhejiang Ocean Monitoring and Forecasting Center, and dataset from 2007 to 2015 is provided by the Zhejiang Ocean Monitoring and Forecasting Center
		2016–2018			monitoring data of 2016–2018 is provided by East China Sea Monitoring Center
Marine hydrometeorology	SST	1981–2018	Shengshan and Nanji stations	specification for coastal observation (GBT 14914–2006)	Daily operational observation data from 1981 to 2018 provided by the East China Sea Forecast Center
	SSTA			sea surface temperature anomaly	
	$SSTA_{10a}$			average SSTA in 10 years	
	ENSO index		Niño3.4 area	monthly mean SSTA in Niño3.4 area	National Oceanic and Atmospheric Administration (https://www.cpc.noaa.gov)
Marine water environment	proportion of class IV to classes less than IV	2000–2018	Zhejiang coastal waters	sea water quality standard (GB 3097–1997)	Zhejiang Marine Environmental Bulletin issued by the Department of Ecology and Environment of Zhejiang Province (http://sthjt.zj.gov.cn.)
Indicators of socio-economic development	gross domestic product (GDP)	1981–2018	Zhejiang Province	added-value index of primary, secondary and tertiary industries	Statistical Yearbook of China issued by the State Statistical Bureau (http://data.stats.gov.cn.)
			Ningbo City	Table 3–2 GDP development index over the years	2019 Ningbo Statistical Yearbook issued by the Ningbo Municipal Statistics Bureau (http://vod.ningbo.gov.cn/)
			Wenzhou City	Table 1–10 GDP development index over the years	2019 Wenzhou Statistical Yearbook issued by the Wenzhou Municipal statistics bureau (http://wztjj.wenzhou.gov.cn.)
	maricultural area	1981–2016	Zhejiang Province	total maricultural area for agriculture	Statistical Yearbook of China issued by the State Statistical Bureau (http://data.stats.gov.cn)

$$R = \sqrt{\frac{U}{S_{yy}}}, \tag{2}$$

mean square error unbiased estimator of the regression equation:

$$\partial = \sqrt{\frac{Q}{n-l-1}}, \tag{3}$$

significance test:

$$F = \frac{U/l}{Q/(n-l-1)} = \frac{R^2/l}{(1-R^2)/(n-l-1)}, \tag{4}$$

where U represents the sum of regressive squares; Q represents the sum of squares of residuals; S_{yy} represents the sum of squares of the total dispersion; n represents the number of samples; and l represents the number of introduced variables or factors.

3 Results

3.1 *Temporal variation*

To understand the multistage temporal variation, the evolution characteristics of red tide over the past 40 years were analyzed and are shown in Fig. 1. The annual occurrences and area of red tide in the Zhejiang coast waters fluctuated year by year. However, three distinct stages, namely, low frequency, explosive growth and fluctuating decline, were exhibited in different time periods. The three stages correspond to the periods from 1981 to 1999, 2000 to 2009 and 2010 to 2018, respectively. The transition point between increasing and decreasing red tide was the year 2003 in the second phase, which reached a peak with a maximum value of 79 in the last 40 a. The inter-annual variability of the red tide area is similar to that of the annual occurrence, although it fluctuates more in the second stage. Since the 21st century, the explosive growth of red tide has made the annual occurrence and area of red tide reach the highest value in history, with an annual average incidence of 45. At the same time, the area increased rapidly to approximately 13.361×10^4 km^2, which is 44 times that in the last century. The annual occurrences reached a historical peak of 79 km^2 times in 2003, while the area increased to 2.734×10^4 km^2 in 2000. After the peak, the number of annual red tide events decreased gradually year by year, but the large-scale red tide events with a large area of more than 1 000 km^2 increased to a total of 24 times in this stage. However, in the third stage after 2010, the annual occurrence and area both declined slowly and showed stable fluctuation, with values significantly lower than those in the previous 10 a. The annual occurrence remained 18 events every year, while the total area of red tide dropped to 1.78×10^4 km^2.

3.2 *Spatial distribution*

In the coastal area of Zhejiang Province, the red tide outbreaks have obvious spatial distribution characteristics of an east-west and north-south trend. Most red tide events in the east-west direction occurred side by side with the coastline and isobaths, 95.4% of which were located to the west of the 50 m isobaths (as illustrated in Fig. 2). A total of 4.2% of the total events occurred between the 50 m and 100 m isobaths. However, due to

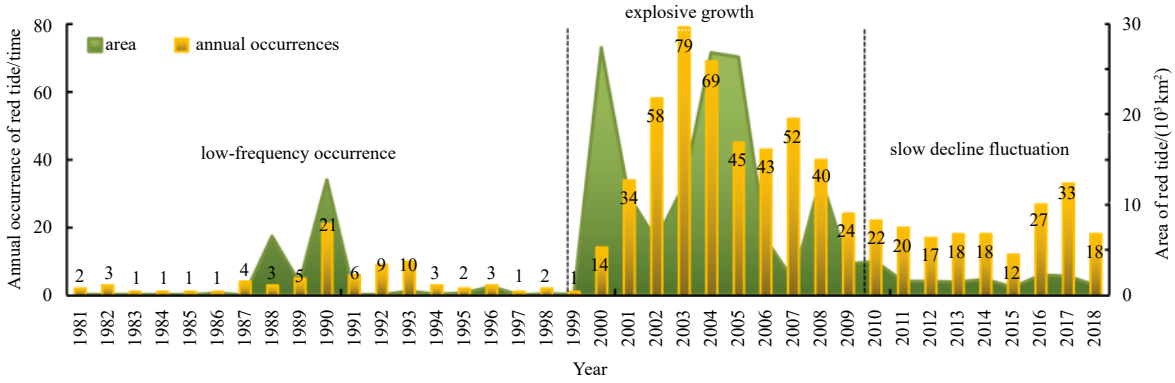

Fig. 1. Annual number and area of red tide events in the Zhejiang coastal waters from 1981 to 2018.

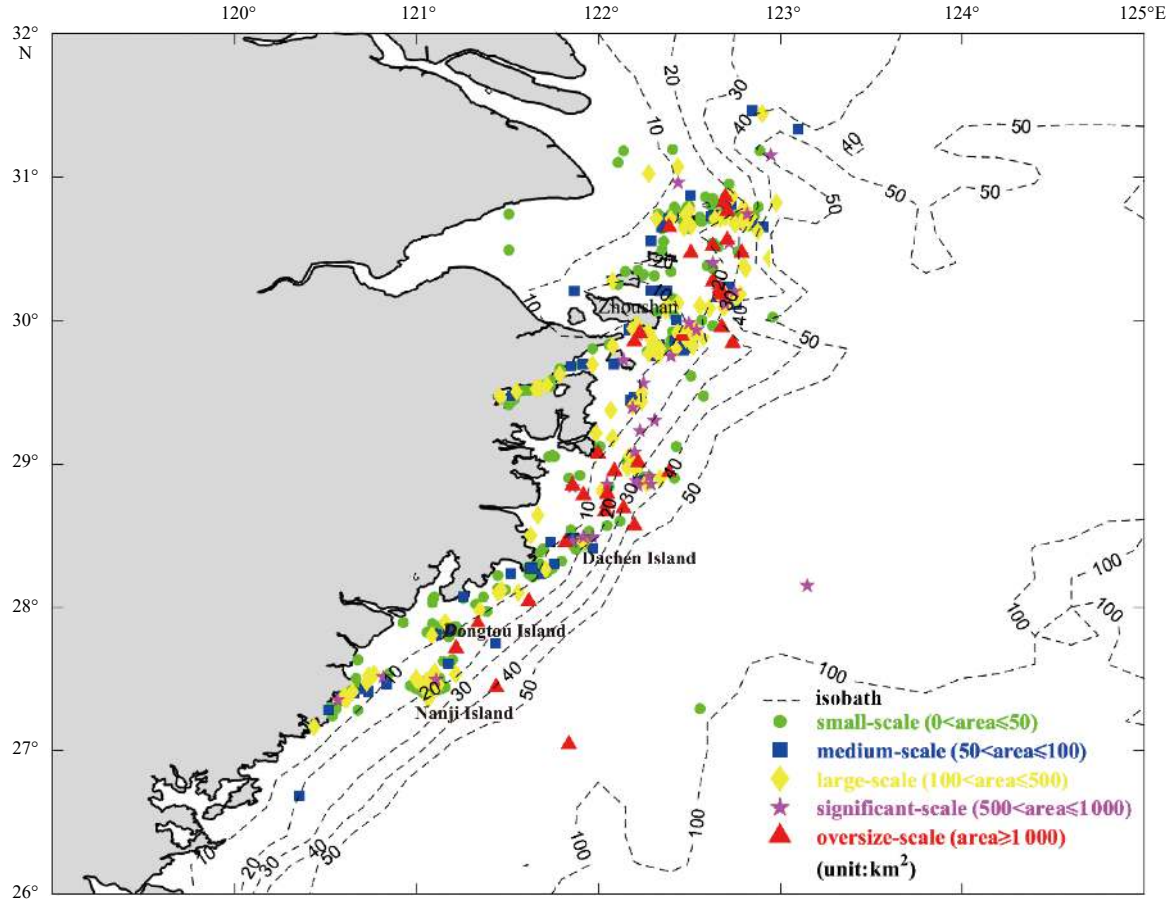

Fig. 2. Red tide distribution in the Zhejiang coastal area over the past 39 years.

the limited nutrient input from the land, only three red tides occurred to the east of the 100 m isobath. The above analysis is basically consistent with a previous study (Cao, 1986). There is a long and narrow submarine slope in the northeast-southwest direction between the 10 m and 50 m isobaths of the Zhejiang coastal waters, and the coastline is actually in line with the isobaric lines and island trends. As a result, the plan-view distribution of nutrients is also in line with the isobaths, which is affected by terrestrial inputs, such as diluted water from the Changjiang River and Qiantang River. The nutrients decrease gradually from the coastal to offshore. Additionally, affected by the coastal current and upwelling, an abnormal structure of inversion and low salinity occurred to the west of the 50 m isobaths along the Zhejiang coastal waters, which can strengthen full vertical mixing and provide the necessary nutrients for a red tide outbreak. Previous studies have shown that the temporal and spatial variation of upwelling is consistent with that of red tide outbreak, which begins in May, intensifies in June, and dissipates gradually from September to October each year (Lou, 2010).

Over the past 39 a, the high-incidence area of red tide in the Zhejiang coastal waters has obviously expanded southward in the north-south direction. Figure 3 shows the frequency of the total red tide occurrences in four coastal cities (as illustrated in Fig. 2) in the three stages, and the change trend of each city is

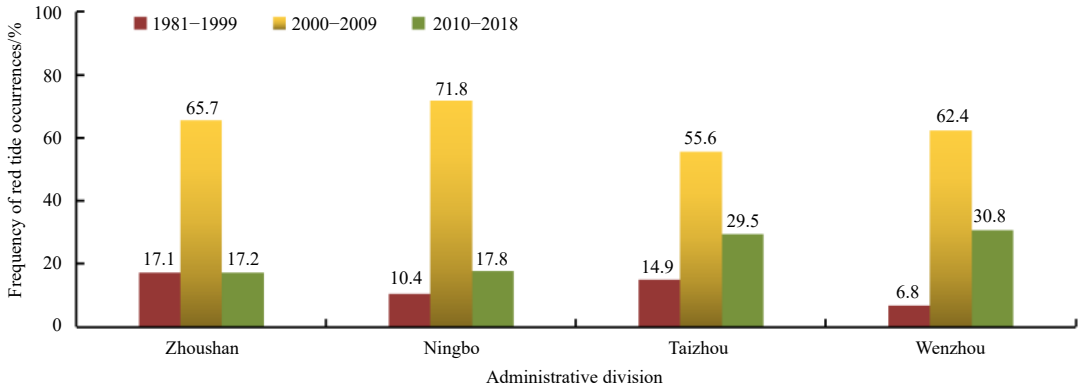

Fig. 3. Red tide occurrence frequency in each decade in coastal cities of Zhejiang Province.

consistent with the three-stage pattern in Fig. 1.

Before the 21st century, the frequency in every city was generally low, while the frequency in Zhoushan was the highest, with a percentage of 17.5%. In the second stage (2000–2009), the frequency showed an upward trend in all the cities, with Ningbo showing the highest at 71.8%. In the third stage (2010–2018), the frequency in all cities began to decrease, but the frequency in Taizhou and Wenzhou continued to increase significantly. The frequency in Taizhou increased by up to 29.5%, and the high-incidence areas gradually shifted from the waters of Sanmen Bay in the 1990s to Dachen Island and Wenling-Shitang in the 21st century. The frequency of Wenzhou increased from the lowest in the first stage to the highest now, which accounts for 30.8%. The above analysis indicates that the high-incidence area of red tide constantly expanded southward in the second and third stages. Additionally, areas such as the Yushan-Jiushan Islands, Dachen Islands, and Dongtou Islands were newly added, in addition to the conventional high-incidence areas of the Zhoushan Islands, Xiangshangang Bay, Sanmen Bay and Nanji Islands.

3.3 *Establishment of a multivariate nonlinear regression equation*

Red tide is a complex ecological anomaly, and previous studies (Mu, 2011; Fu et al., 2012) have shown that eutrophication provides the material basis and necessary conditions for red tide. Land-based emissions and mariculture are the main sources of nutrients. The occurrences of red tide and the succession of biological populations are regulated by hydrological and meteorological conditions at different temporal and spatial scales. Therefore, nutrient and hydrometeorological conditions are considered simultaneously in this paper. We introduce seven factors, namely, the sea surface temperature (X_{sst}), mariculture area (X_{mar}), growth rate of primary industry (X_{pri}), growth rate of secondary industry (X_{sec}), growth rate of tertiary industry (X_{ter}), ENSO index ($X_{Niño3.4}$), and proportion of water quality class IV to classes less than IV (X_{wq}). The statistical analysis and physical mathematical model were adopted to analyze the main factors influencing the annual occurrence of red tide (Y_{AORT}) in different stages. In addition, we conducted causal analysis and provided a mechanistic discussion of the inter-annual variation and southward expansion.

First, all the datasets were analyzed by SPSS, and a histogram with a normal curve was drawn to determine whether the data had a bell-shaped distribution. Second, the skewness and kurtosis were calculated, and the nonparametric Shapiro-Wilk (W) test was adopted. The results indicate that X_{sst}, $X_{Niño3.4}$, X_{mar}, and X_{wq} exhibit normal or partial normal distributions and that Y_{AORT}, X_{pri}, X_{sec}, and X_{ter} exhibit non-normal distributions (Table 2). In scenarios where certain dependent variables diverged from the normal distribution or the overall distribution was unknown, the Spearman correlation coefficient was used to analyze the correlation between Y_{AORT} and the impact factors in this study. It was found that the factors X_{sst}, X_{mar}, X_{pri}, X_{sec}, and X_{ter} were positively correlated with Y_{AORT}, among which the correlation coefficient between X_{mar} and Y_{AORT} was the highest at 0.743 (Table 3).

Among the nutrient indexes, moderate positive correlations existed between X_{mar}, X_{sec} and Y_{AORT}, while low positive correlations existed between X_{pri}, X_{ter} and Y_{AORT}. Hence, X_{mar} and X_{sec} were selected as the representative indicators. Although $X_{Niño3.4}$ had no significant correlation with Y_{AORT} based on the 39 a time-series dataset, the correlation between X_{sst} and Y_{AORT} in the Zhejiang coastal waters increased, with a correlation coefficient of 0.326. Thus, X_{sst} was selected as the representative temperature indicator.

Because any function can be approximated by polynomials within an appropriate range, the regression equation is suitable for the analysis through adjusting the degree of a polynomial. In this study, based on the multivariate nonlinear regression process provided by SPSS, a mathematical model considering $X_{mar,}$ $X_{sec,}$ and X_{sst} was established by curve fitting and the iterative calculation by adopting the Levenberg-Marquardt estimation method. The specific equations are shown below:

$$Y_{AORT} = \frac{1}{3}\left(-1\,307.87 + 195.54X_{sst} - 95.83X_{sst}^2 + 1.54X_{sst}^3\right) + \frac{1}{3}e^{(0.124X_{mar}-9.573)} + \frac{1}{3}\left(-3.096X_{sec} + 0.682X_{sec}^2 - 0.016X_{sec}^3\right). \quad (5)$$

The goodness of fit coefficient of this equation is 0.907, indicating that the proportion of variables that can be explained by the independent variables in the total variation of the dependent variables is as high as 90.7% (Table 4), which can be used to conduct causal analysis and provide a mechanistic discussion of the spatiotemporal variation and southward expansion of red tide events.

4 Discussion

4.1 *Effects of environmental changes and human activities on red tide occurrence*

The difference in the influence of the local SST and ENSO teleconnection on red tide outbreak is significant. Although pre-

Table 2. Nonparametric test statistics of the normal distributions of red tide occurrence and factors

Factor	Shapiro-Wilk			Skewness	Kurtosis
	Statistics	Freedom	Significance	Statistics	Statistics
Y_{AORT}	0.835	38	0	1.34	1.215
X_{SST}	0.957	38	0.147*	0.365	–0.344
$X_{Niño3.4}$	0.985	38	0.881*	0.257	–0.339
X_{mar}	0.923	36	0.015*	0.3	–1.416
X_{wq}	0.96	19	0.572*	0.577	–0.264
X_{pri}	0.886	38	0.001	0.674	–0.838
X_{sec}	0.814	38	0	0.924	–0.633
X_{ter}	0.763	38	0	1.44	1.051

Note: * When the significance is >0.05, the factor exhibits normal or partially normal distributions.

Table 3. Rank correlation coefficient of red tide occurrence and factors

	Variable	Y_{AORT}	SST		Nourishment				Water quality
			X_{SST}	$X_{Niño3.4}$	X_{mar}	X_{pri}	X_{sec}	X_{ter}	X_{wq}
	Code	7	1	8	2	3	4	5	6
Y_{AORT}	correlation coefficient	1	0.326*	0.107	0.743**	0.394*	0.696**	0.461*	0.22
	Sig (two-sided)	–	0.046	0.524	0	0.016	0	0	0.366
	N	38	38	38	36	37	37	37	19

Note: * When the confidence coefficient (two-sided test) is 0.05, the correlation is significant; ** when the confidence coefficient (two-sided test) is 0.01, the correlation is significant; – represents no data.

Table 4. ANOVA of the multivariate nonlinear regression equation

Source	Sum of squares	Degrees of freedom	Mean square
Regression	26 504.633	9	2 944.959
Residual	1 410.367	26	54.245
Total before correction	27 915	35	
Total after correction	15 127.543	34	

Note: R^2=1–(residual sum of squares)/(corrected sum of squares) = 0.907.

vious studies (Deng et al., 2017; He and Yang, 2009) revealed that the annual occurrence of red tide is correlated with the ENSO index, they have not discussed the three distinct inter-annual stages of red tide in the Zhejiang coastal waters. In this paper, the data analysis shows a high correlation (r=0.85, p=0.01) between Y_{AORT} and $X_{Niño3.4}$ from 2000 to 2009, a moderate correlation (r=0.55, P=0.05) between these factors from 2010 to 2018 and a weak correlation (r=0.31, p=0.05) between them from 1981 to 1999. These findings are consistent with the strong correlation reported between Y_{AORT} and $X_{Niño3.4}$ over a certain period of time (He and Yang, 2009). Moreover, $X_{Niño3.4}$ was not significantly correlated with Y_{AORT} based on the 39-year time-series dataset, although the correlation between X_{sst} and Y_{AORT} in the Zhejiang coastal waters increased, with a correlation coefficient of 0.326. The variation characteristics of $SSTA_{10a}$ in the three stages were consistent with that of red tide events, with correlation coefficients as high as 0.7. As shown in Fig. 4, the local $SSTA_{10a}$ increased in steps from 1981 to 2009, reached a peak value of 0.36°C in the second stage (2000–2009) and decreased to 0.002°C in the third stage (2010–2018). These findings indicated that the influence of SSTs on the annual occurrence of red tide can be revealed over an interdecadal-scale period. However, the local SST was more representative because the effect of El Niño on the local SST in the Zhejiang coastal waters presented a lag of 8 to 10 months via the teleconnection (Zhong et al., 2004).

In addition to natural environmental factors, human activities also play a key role in the outbreak of red tides. Figure 5 shows a comparison of two fitting values to quantitatively analyze the contribution of each factor. In this case, Y_1 is the fitting value obtained by comprehensively considering X_{sst}, X_{mar}, and X_{sec}, with a goodness of fit coefficient of 0.907; Y_2 is the fitting value in which only X_{sst} and X_{mar} are considered, and the goodness of fit coefficient is 0.687. The values of Y_2 in 2006, 2007 and 2011 were obviously smaller than that of Y_1. It is noteworthy that the mariculture areas in 2006 and 2007 decreased to approximately half of that in 2005, with a value of 60×10^4 km^2. Additionally, the SST suddenly decreased from 17.33°C in 2010 to 16.8°C in 2011, while the mariculture area was stable. However, it is interesting to note that the growth rate of the secondary industry increased from 13.27% in 2005 to 19.54% in 2006 and 23.84% in 2007, and it increased suddenly to 32.76% in 2011. Thus, the fitting value Y_1, in which X_{sec} was considered, is highly consistent with the actual value (Fig. 5). Therefore, 68.7% of the variation in the annual red tide occurrence was due to the SST and mariculture area; however, secondary industry growth could compensate for the nutrient deficiency caused by the sharp mariculture area reduction and SST decline.

4.2 *Analysis of the inter-annual variation and southward expansion of red tides*

We can provide a detailed account of the main controlling mechanism of the distinct inter-annual variation rule of red tide in three stages based on the regression model of Y_1 from the perspective of nutrient supply and SST changes. From 1981 to 1999, the Zhoushan sea area had the most red tide events, which may be related to the abundant nutrients brought by the fresh water of the Changjiang River, while the central Zhejiang sea area had fewer red tide occurrences. During this period, the mariculture

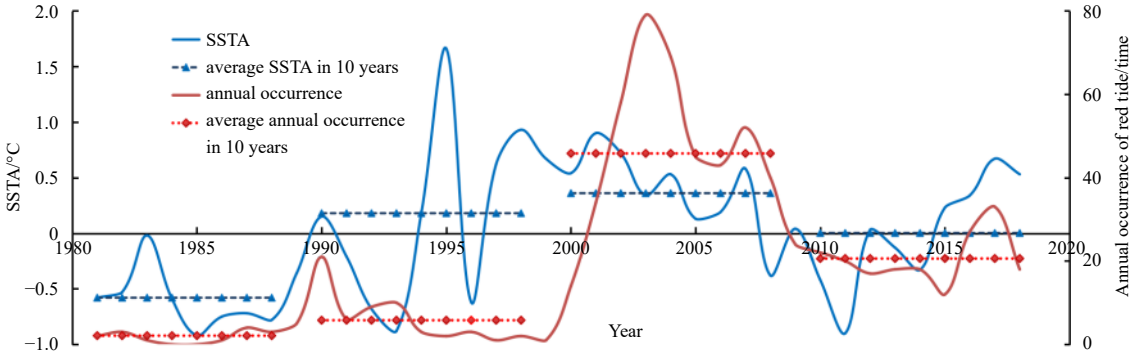

Fig. 4. Relationship between the annual occurrence of red tide and the SSTA

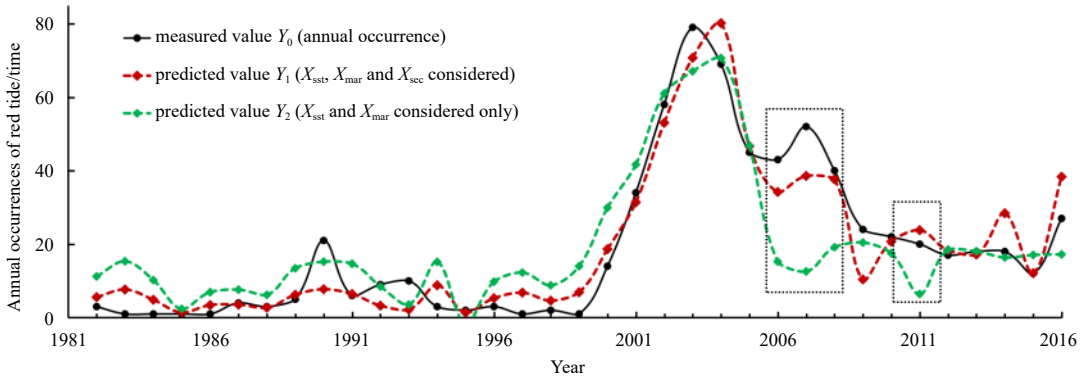

Fig. 5. Comparison of simulated and actual values of the nonlinear regression equation.

area maintained a slow growth rate of less than 2%, and the growth rate of the secondary industry was less than 7%. The annual occurrences of red tide fluctuated between 2 and 5 times in most years. However, the first small peak was 21 times, which occurred in 1990. Because the local SST rose to 17.9°C in 1990, which was the highest value between 1981 and 1993, we can conclude that the local SST was the main controlling factor in this low-frequency stage.

After the 21st century, the obvious "roller coaster" structure of red tide occurrence appeared (Fig. 1). The occurrence of red tide increased sharply and reached a historical peak of 79 times in 2003 and then declined quickly. The annual average was 45.8 times per year. The high-incidence areas of red tide gradually spread from the northern to the central and southern areas of Zhejiang coastal waters. The large-scale red tide events broke out frequently, and six large-scale red tides with an area of 3 000 km^2 or more occurred from 2001–2005. These red tides mainly broke out in the upwelling area, which was distributed between 122°E and 124°E longitude within the 30 m to 50 m isobaths, and they exhibited a sinuous and swinging strip-like pattern that paralleled the coastlines. The local SST maintained a positive anomaly and rose rapidly during the same period. SST_{10a} reached 18.11°C, which was the highest value to date. The mariculture area gradually expanded from 9.7×104 km^2 in 1981 to 118.3×104 km^2 at the peak in 2004. Environmental pollution was caused by the agglomeration and development of coastal cities in Zhejiang. As a result, the proportion of water quality class IV to classes less than IV increased, reaching a peak of 85.7% in 2002. Moreover, studies have shown that in the past 30 years, the PDO (Pacific Decadal Oscillation) changed from low value to high value in the late 1990s, which led to a stronger Kuroshio intrusion and enhanced coastal upwelling (Cloern et al., 2007). The East Asian summer monsoon also showed an increasing trend at the interdecadal scale, especially after 2000, which led to stronger atmospheric convergence of the surface layer (925 hPa) along the coast of Zhejiang-Fujian; moreover, the convective activity was intensified, the cyclonic vorticity was enhanced, and the coastal upwelling was strengthened (Xu et al., 2013). The enhancement of upwelling increased the nutrient concentration (Wooster and Zhang, 2004), which promoted the outbreak of red tide. The unique period of large-scale and frequent outbreaks of red tide occurred because of the combined effect of the abundant nutrient supply and appropriate hydrological and meteorological conditions. However, the ecological effects caused by ocean-atmosphere interactions and climate change should be thoroughly investigated.

In the third stage (2010–2018), the SST decreased slightly and showed a negative anomaly and SST_{10a} decreased to 17.75°C. The mariculture area decreased slightly but remained stable over 86×10^4 –93×10^4 km^2. Although the net value of secondary industry production continued to increase, the growth rate slowed down. Moreover, all types of land-based pollution emissions were effectively controlled due to environmental protection programs, such as "clear water and green mountains". Consequently, the annual occurrence of red tide decreased significantly and remained at a stable level of approximately 20 times per year. Small and medium-sized red tide events accounted for the majority and the southward expansion of high-incidence areas was still obvious. Since 2008, the frequency of red tide was higher in Wenzhou than in Ningbo. Figure 6 shows that the variation tendency of SST in the Wenzhou and Ningbo coastal areas were the same, with a stable difference of 1.4°C, while the difference in

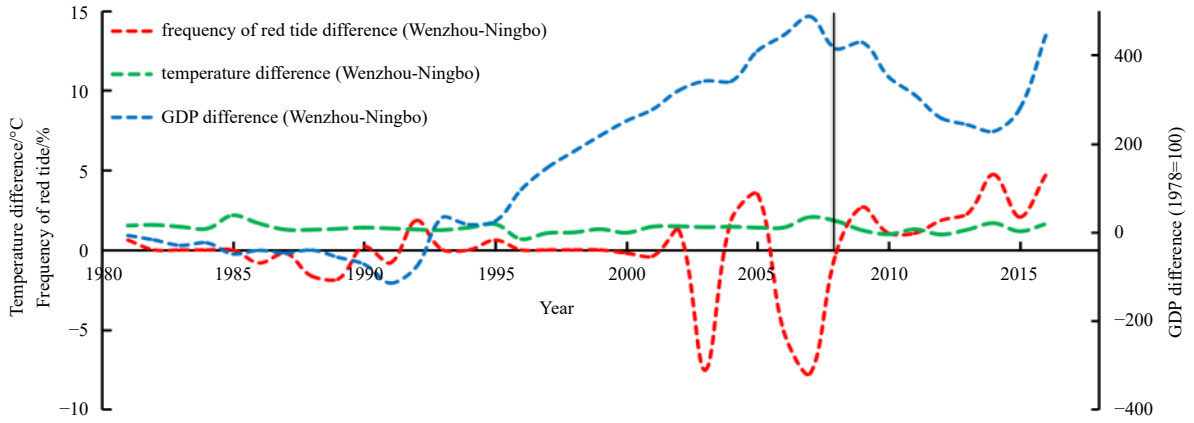

Fig. 6. Analysis of the mechanism of the southward expansion of red tide.

GDP between the two cities changed dramatically. Before 1992, the GDP index of Wenzhou was significantly lower than that of Ningbo, and the maximum difference was –114.9. After 1992, Wenzhou's economy developed rapidly and has surpassed that of Ningbo City, with the difference reaching the maximum value of 487 in 2007. In particular, the index difference of the secondary industry increased from –84.4 in 1989 to 6 447.4 in 2014. The rapid economic development of southern cities, especially the secondary industry of these cities, inevitably led to an increase in land-based pollution emissions, which was one of the reasons for the continuous southward expansion of high-incidence areas. Over time, the nutrients carried by the runoff of the Changjiang River and Qiantang River were continuously transported to the south by the Zhejiang-Fujian Coastal Current (ZFCC) and deposited in the southern muddy sea area, resulting in the continuous accumulation of nutrients at the bottom, which may also partially explain the southward expansion of the high incidence area.

5 Conclusions

Based on a 39-year time series dataset from 1981 to 2018 in the Zhejiang coastal waters, a distinct inter-annual variation pattern with three stages, namely, low frequency, explosive growth and fluctuating decline, was found. In addition, 95.4% of the red tide events occurred in the upwelling area to the west of the 50 m isobaths. The southern expansion trend of the high-frequency area was obvious. Seven factors related to nutrient and hydrometeorological conditions were analyzed via a Spearman's correlation analysis, and the mariculture area, secondary industry growth rate and local SST were identified as the main impact factors. In addition, a multivariate nonlinear regression model with a fit coefficient as high as 0.907 was established to identify the reason for the temporal-spatial variations. The results showed that 68.7% of the variation in the annual occurrence of red tide was due to the SST and mariculture area and that secondary industry growth could compensate for the nutrient deficiency caused by the sharp reduction of mariculture area and decline of SST. In the low-frequency period of the 1980s and 1990s, the local SST was the main controlling factor under the extremely low mariculture area level and secondary industry growth rate. In the second stage (2000–2009), the three impact factors all reached peak values while the POD and East Asian monsoon continued to strengthen after 2000, which led to the enhancement of upwelling. As a result, the annual occurrences of red tide exceeded the historical extreme value, with frequent occurrences of large-scale and toxic red tides. In the third stage (2010–2019), remarkable achievements in economic structural transformation and environmental protection, such as the "clear water and green mountains" program, led to a decrease in the absolute number of annual occurrences by at least half. However, an obvious southward expansion of high-incidence areas has occurred since 2010, and the preliminary analysis results showed that the rapid development of secondary industry in coastal cities of southern Zhejiang was the main factor.

Acknowledgements

We thank Xiulin Lou of the Second Institute of Oceanography (MNR) for the guidance and the valuable suggestions on the revision. We are also grateful to the anonymous reviewers for their helpful comments on the manuscript.

References

Cao Xinzhong. 1986. Prelimary study on the seasonal process of the coastal upwelling off Zhejiang in the east Sea, China. Journal of Fisheries of China (in Chinese), 10(1): 52–68

Chen Yanlong, Yang Jianhong, Zhao Dongzhi, et al. 2013. Quantitative study on effect of seawater temperature on specific growth rate of algal species. Marine Environmental Science (in Chinese), 32(1): 104–110

Cloern J E, Jassby A D, Thompson J K, et al. 2007. A cold phase of the East Pacific triggers new phytoplankton blooms in San Francisco Bay. Proceedings of the National Academy of Sciences of the United States of America, 104(47): 18561–18565, doi: 10.1073/pnas.0706151104

Deng Bangping, Zhang Haofei, He Yanlong, et al. 2017. Analysis on the relationship between the red tide events and El Niño in the East China Sea from 1981 to 2011. Ecological Science (in Chinese), 36(6): 161–164

Feng Jianfeng, Wang Hongli, Li Shengpeng. 2007. Research on prediction of phytoplankton's density using support vector machines. Marine Environmental Science (in Chinese), 26(5): 438–441

Fu Mingzhu, Wang Zongling, Pu Xinming, et al. 2012. Changes of nutrient concentrations and N: P: Si ratios and their possible impacts on the Huanghai Sea ecosystem. Acta Oceanologica Sinica, 31(4): 1001–112

Guo Hao, Ding Dewen, Lin Feng'ao, et al. 2015. Characteristics and patterns of red tide in china coastal waters during the last 20a. Advances in Marine Science (in Chinese), 33(4): 547–558

Gao Junzhang, Liu Yalin, Lin Yi, et al. 2017. Analysis on characteristics of red tide disaster in Wenzhou coastal waters during the last 10 years. Transactions of Oceanology and Limnology (in Chinese), (4): 86–90

He Chunliang, Yang Hong. 2009. Space-time distribution of red tide events in China and its relationship with the El Niño. Journal of Shanghai Ocean University (in Chinese), 18(2): 206–211

Jing Zhiyou, Qi Yiquan, Hua Zulin. 2008. Numerical study on summer upwelling over northern continental shelf of South China Sea. Journal of Tropical Oceanography (in Chinese), 27(3): 1–8

Li Xueding. 2012. Analysis on characteristics of red tide in Fujian coastal waters during the last 10 years. Environment Science (in Chinese), 33(7): 2210–2216

Lin Jun. 2011. A modeling study of the phytoplankton dynamics off the Changjiang estuary (in Chinese) [dissertation]. Shanghai: East China Normal University

Liu Lusan, Li Zicheng, Zhou Juan, et al. 2011. Temporal and spatial distribution of red tide in Yangtze River Estuary and adjacent waters. Environmental Science (in Chinese), 32(9): 2497–2504

Long Hua, Zhou Yan, Yu Jun, et al. 2008. Analyses on harmful algal blooms in Zhejiang coastal waters from 2001 to 2007. Marine Environmental Science (in Chinese), 27(S1): 1–4

Lou Xiulin. 2010. Remote sensing observation of upwelling current in Zhejiang coastal waters and the relationship between red tide (in Chinese) [dissertation]. Qingdao: Ocean University of China

Mu Di. 2011. The study on the ecological water quality dynamic modeling of Bohai bay (in Chinese) [dissertation]. Tianjin: Tianjin University

Qi Yuzao. 2003. Red Tide Along the Coast of China. Beijing: Science Press, 3–5

Song Nanqi, Wang Nuo, Wu Nuan, et al. 2018. Temporal and spatial distribution of harmful algal blooms in the Bohai Sea during 1952–2016 based on GIS. China Environmental Science (in Chinese), 38(3): 1142–1148

Wang Hongli, Ge Gen, Li Yuelei. 2006. Research on the prediction of red tide based on the Fuzzy Neural Network. Marine Science Bulletin (in Chinese), 25(4): 36–41

Wei Guiqiu, Wang Hua, Cai Weixu, et al. 2012. 10-year retrospective analysis on the harmful algal blooms in the Pearl River Estuary. Marine Science Bulletin (in Chinese), 31(4): 466–474

Wen Shiyong, Zhao Dongzhi, Zhao Ling, et al. 2009. Tolerance response model of N/P ratios for red tide algae. Journal of Dalian Maritime University (in Chinese), 35(1): 118–122

Wooster W S, Zhang C I. 2004. Regime shifts in the North Pacific: early indications of the 1976–1977 event. Progress in Oceanography, 60(2–4): 183–200, doi: 10.1016/j.pocean.2004.02.005

Xu Lili, Gong Maoxun, Xu Tingting, et al. 2013. Relationships between the east Asian monsoon anomalous and the red tide occurrence frequency in the East China Sea mental factors in the Beidaihe waters of the Qinhuangdao. Marine Forecasts (in Chinese), 30(5): 8–14

Yang Hong, He Chunliang. 2009. The red tide events in the China Sea and the relationship with the temperature and El Niño. Transactions of Oceanology and Limnology (in Chinese), 2(2): 1–6

Zhang Qingtian. 2013. Review on the annual variation of red tides in China Sea. Environmental Monitoring in China (in Chinese), 29(5): 98–102

Zhao Dongzhi. 2010. The Occurrence Regularity of Red Tide Disasters in the Typical Waters of China (in Chinese). Beijing: China Ocean Press

Zhao Dongzhi, Zhang Fengshou, Zhao Ling. 2003. Detecting chlorophyll and hazard algal bloom in coastal water with normalized deference of AVHPP. Ocean Technology (in Chinese), 22(3): 30–33

Zhao Dongzhi, Zhang Fengshou, Yang Jianhong, et al. 2005. The optimized spectral bands ratio for the relation of sun-induced chlorophyll fluorescence height with high chlorophyll *a* concentration of algal bloom waters. Haiyang Xuebao (in Chinese), 27(6): 146–153

Zhong Shanshan, He Jinhai, Liu Xuanfei, et al. 2004. Possible mechanisms of Enso's decadal variability. Journal of Tropical Oceanography (in Chinese), 23(2): 28–36